Glasnik hemičara i tehnologa Bosne i Hercegovine

Bulletin of the Chemists and Technologists of Bosnia and Herzegovina

2026

66

31-40

Print ISSN: 0367-4444
Online ISSN: 2232-7266

Original Scientific Article
DOI: 10.35666/2232-7266.2026.66.04
UDK: 543.31:541.1

Bentonite as an adsorbent for the removal of Cr(III) ions from galvanic wastewater: equilibrium, kinetics and thermodynamics in batch and column systems

Ahmetović, M.*, Šestan, I., Odobašić, A., Papraćanin, E., Keran, H., Junuzović, H.

Faculty of Technology, University of Tuzla, Urfeta Vejzagića 8, 75000 Tuzla, Bosnia and Herzegovina

Article info
Received: 21/11/2025
Accepted: 04/02/2026

Keywords:
Bentonite
Chromium
Galvanic wastewater
Adsorption
Batch system
Column

***Corresponding author:**
Melisa Ahmetović
E-mail: melisa.ahmetovic@untz.ba
Phone: +-387 35 320 768

Abstract: The presence of heavy metals such as chromium in waterways can lead to various health problems in humans and animals. Due to its negative effects, chromium-rich wastewater needs to be treated before being discharged into waterways. In this study, the possibility of using bentonite as an adsorbent for the removal of Cr (III) from galvanic wastewater was investigated. First, the physicochemical characterization of the used bentonite was performed, followed by the examination of process parameters such as pH value, concentration, mass, and time. Based on the obtained data, adsorption isotherms, kinetic models, and thermodynamic parameters were determined. All experiments were carried out in both batch and column systems. The results showed that bentonite can be used as a low-cost adsorbent for the efficient removal of chromium ions from galvanic industry wastewater, achieving the highest removal efficiency (99.97%) at pH 5 and a mass of 1 g. The Langmuir and Temkin adsorption isotherm models showed good agreement with the experimental data ($R^2 > 0.9$), while the best fit for the kinetic study was observed with the pseudo-first-order model.

INTRODUCTION

Industrial wastewater often contains heavy metals such as copper, zinc, chromium, lead, nickel, cadmium, and others, which pose a serious problem for the entire ecosystem (Ahmetović *et al.,*2024). For the successful implementation of the galvanization process, as one of the industrial processes, the electrolyte must contain metal ions as direct components of the galvanic bath. Therefore, during the galvanization process, galvanic wastewater becomes contaminated with heavy metals, which represent a direct threat to human health. Chromium, as one of the common components of galvanic baths, although considered an essential element necessary for the proper functioning of living organisms, can cause respiratory irritation, liver and kidney damage, and even cancer when present in concentrations exceeding the permissible limits (Gaoqian *et al.*,2024).Chromium exists in two valence states, as trivalent and hexavalent chromium ions (Dengbing *et al.,*2025). The trivalent ion appears in water in the form of Cr(III) complexes and hydrogen–oxygen complexes, whereas the hexavalent chromium ion exists in the form of ionic oxides (Wael *et al.*,2023). In order to minimize their concentrations, various methods for the removal and treatment of heavy metals have been developed in recent years (Kejin *et al.,*2025). The selection of an appropriate method for removing heavy metals from galvanic wastewater primarily depends on the type of contaminant. Among numerous methods, adsorption has attracted considerable attention due to its high availability, simplicity, selectivity, and efficiency (Joyel *et al*.,2024). In addition, adsorption can remove different types of pollutants, which makes it increasingly used in wastewater treatment processes (Ahmetović *et al.,*2024). In recent years, clays, zeolites, activated carbon, and similar materials have been increasingly used as adsorbents for the removal of heavy metal ions (Sher *et al.,*2021). A large specific surface area, high ion-exchange capacity, flexibility, and unique physical properties are some of the main advantages of clay materials (Gholamifard *et al*.,2023). Bentonite clays belong to the montmorillonite group and are characterized by very high chemical and mechanical stability, as well as diverse surface and structural properties, making them inexpensive and

environmentally friendly adsorbents for the removal of heavy metals (Tadesse,2022). Therefore, the aim of this study was to investigate the possibility of using bentonite clay for the removal of chromium ions from galvanic wastewater using both batch and column systems, in order to optimize the use of bentonite clay for Cr(III) ion removal from galvanic wastewater and to assess its potential for large-scale application.

EXPERIMENTAL

Bentonite from the Šipovo locality (Bosnia and Herzegovina) with a particle size of 75 μm was used in this study. The physicochemical characterization included the determination of the cation exchange capacity, specific surface area, point of zero charge, and the performance of SEM-EDS and FTIR analyses. The cation exchange capacity was determined using the standard 1 mol/L NH_4Cl method, while the point of zero charge (pH_{pzc}) was determined using 0.1 mol/L $NaNO_3$ as the electrolyte (Daković,2001). The specific surface area was measured by nitrogen adsorption at 77 K using a Micromeritics Tristar II Plus Analyzer, Malvern Panalytical and the surface area value of the sample was calculated using the standard Brunauer–Emmett–Teller (BET) method. The surface topography and chemical composition of the bentonite were analyzed using a JSM–6460LV, JEOL scanning electron microscope equipped with energy-dispersive X-ray spectroscopy (SEM-EDS) at an accelerating voltage of 20 kV, while functional groups were identified using an ABB Bomem MB-100 Fourier Transform Infrared Laboratory Analyzer, Bomem Inc. in the spectral range of 4000–400 cm^{-1} with a resolution of 2 cm^{-1}.

Biosorption experiments were performed using a synthetic solution and a real sample taken from the galvanic industry after metallization/chromium plating. All experiments were performed in triplicate. Synthetic solutions of different concentrations were prepared by dissolving $CrCl_3 \cdot 6H_2O$, Carlo Erba, in distilled water. This salt is pure analytical grade (p.a.>99%). The pH was adjusted by adding 0.1 mol/L and 0.01 mol/L HNO_3 and NaOH solutions. To determine the optimal adsorption conditions, the adsorbent mass of 0.5 g to 2.5 g was used, as well as contact time of 5 min to 60 min, solution initial pH of 2 to 6, temperature of 25ºC to 45°C, and initial metal ion concentration of 10 mg/L to 10000 mg/L. Adsorption was tested in the batch system by mixing 1 g of bentonite with 50 mL of the test solution on a magnetic stirrer at 300 rpm for a specified contact time. After adsorption, the solutions were filtered, and the residual concentration of chromium ions in the filtrate was determined using atomic absorption spectrometry with a Perkin Elmer AAnalyst 200 spectrophotometer (Wu,2019). The adsorption capacity q_e (mg/g) and the metal ion removal efficiency E (%) were calculated using the following equations (Saghir *et al*.,2025):

$$q_e\left(\frac{mg}{g}\right) = \frac{(c_0 - c_e)\cdot v}{m} \quad (1)$$

$$E\ (\%) = \frac{(c_0 - c_e)}{c_0}\cdot 100 \quad (2)$$

where: C_0(mg/L) – initial metal concentration, C_e(mg/L) – equilibrium metal concentration, V– volume of the solution (L), m– mass of the used adsorbent.

To obtain the breakthrough curve, the experiments were carried out in a plexiglass column with a diameter of 30 mm and a height of 230 mm. Before introducing the metal ion solution, the adsorbent was washed with a certain amount of distilled water to remove dissolved compounds. After washing and draining the column, the experiment was continued using both synthetic and real metal ion solutions. The column adsorption experiments were performed in a single-pass mode, and the effluent was collected in portions of 100 mL, after which the metal concentration in each effluent sample was determined.

RESULTS AND DISCUSSION

The point of zero charge (pH_{pzc}) was determined using the salt addition method, with $NaNO_3$ used as the electrolyte. The determined point of zero charge value for the bentonite was 9, indicating that the surface of the adsorbent is positively charged at pH values below this point, thereby attracting anions, while at pH values above this point, the surface becomes negatively charged and attracts cations (Noreen *et al*.,2021; Dhaouadi *et al.,*2021). The total exchange of all cations (CEC), determined by the standard method using 1 mol/L NH_4Cl, was 0.6147 mmol/g, which represents a slightly lower value compared to the CEC of smectites (0.80–1.50 mmol/g). This is due to the presence of non-clay materials in the bentonite structure alongside montmorillonite (Vhahangwele, 2014). Based on the obtained results, it can be concluded that Na^+ ions are dominant compared to other metals, indicating that Na^+ ions from bentonite are likely to be exchanged with Cr(III) ions through an ion-exchange mechanism. According to the results presented in Table 1, it can be concluded that after Na^+ ion, the following order of ion exchange is expected $Ca^{2+} < Mg^{2+} < K^+$.

Table 1: Cation exchange capacity (CEC) value of bentonite

Exchangeable cations	Value (mmol/g)
Ca^{2+}	0.180
Mg^{2+}	0.043
K^+	0.011
Na^+	0.380

The specific surface area of bentonite was 80.9976 m^2g^{-1}, with a pore volume of 0.064904 cm^3g^{-1} and an average pore diameter of 32.052 Å (Table 2). Similar values of specific surface area for bentonite used as an adsorbent were obtained by Kovo (2015), who used Nigerian bentonite for the removal of Ni(II) and Mn(II) ions (69.34 m^2g^{-1}), and by Petrović *et al.* (2019), who used natural bentonite for the removal of Cr(VI) ions (88.80 m^2g^{-1}).

Table 2: Values of the specific surface area of bentonite

Characteristics	Value
BET specific surface	80.9976 m^2g^{-1}
Pore volume (p/p°=0.95)	0.0649 cm^3g^{-1}
Average pore width	65.922 Å
Average pore diameter	32.052 Å

SEM-EDS micrographs are shown in Figure 1 and Figure 2, illustrating the changes in the surface structure of the adsorbent before and after adsorption of Cr(III) ions.

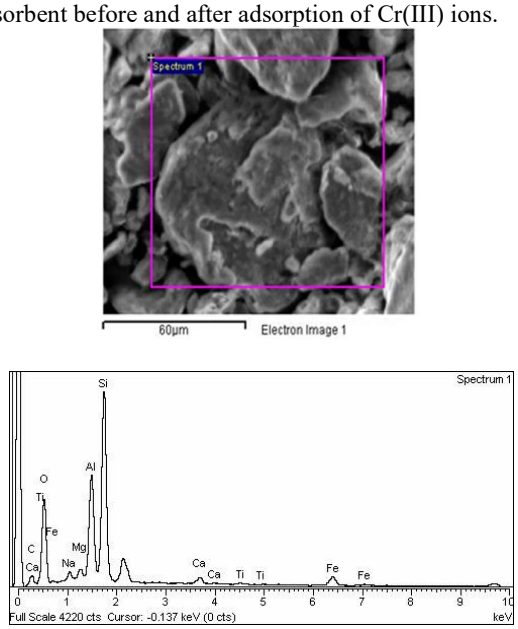

Fig 1. SEM-EDS image of native bentonite

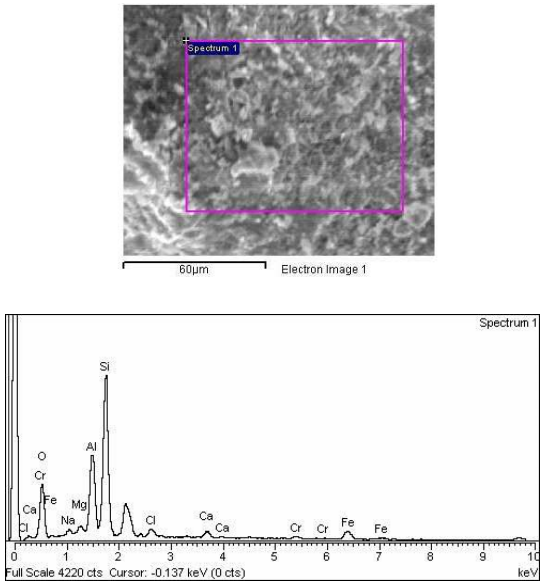

Fig 2. SEM-EDS image of bentonite after adsorption of Cr(III) ions

The morphology of the native sample showed a surface with clearly visible large cavities and macropores of randomly irregular orientation. Such a material structure is an essential prerequisite for the adsorption of heavy metals. Figure 2. shows that, after adsorption with Cr(III) ions, structural changes occurred in the bentonite, indicating that adsorption is associated with chemical alterations, which was further confirmed by FTIR analysis. The results of the SEM-EDS analysis of the native sample showed a significant mass percentage of C, O, Al, and Si, while the SEM-EDS analysis of the bentonite sample after Cr(III) ion adsorption indicated the incorporation of w(Cr)=0.97%, w(O)=47.50%, w(Si)=27.57%, w(Al)=12.59% , w(Na)= 1.67%, w(Ca)= 1.50 % and the absence of C ions. IR spectra were recorded in the range of 4000 to 400 cm^{-1}, and Figure 3. (a and b) shows the spectra of the bentonite samples before and after the adsorption process.

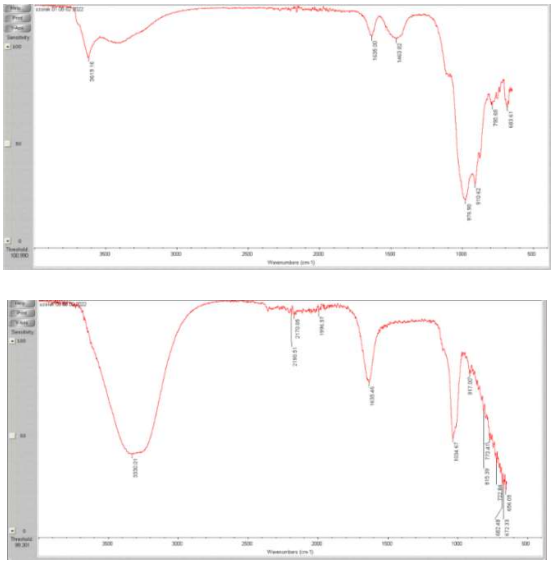

Fig 3. a) FTIR analysis of the native bentonite sample, b) FTIR analysis of the bentonite sample after adsorption of Cr(III) ions

The analysis of the native bentonite sample showed that the first peak appears at 3619.16 cm^{-1}, corresponding to the stretching vibrations of –OH groups that are part of the octahedra where Al^{3+} ions are coordinated with 6 –OH groups, which is typical for dioctahedral smectites. The peak observed at 1635 cm^{-1} is attributed to the bending vibrations of the H–O–H group, corresponding to water molecules located between the layers of the silicate matrix. The peak at 1463.82 cm^{-1} corresponds to the vibrations of the –OH group, while the peaks appearing in the range of 1400–800 cm^{-1} indicate the stretching vibrations of the Al–OH and Si–OH groups, suggesting that the bentonite composition likely contains quartz as an additive (Fonseca *et al*.,2006). Similar FTIR values were obtained by Maged *et al.* (2020) and Gandhi *et al.* (2022), who used bentonite for the removal of heavy metal ions. The FTIR analysis after adsorption of Cr (III) ions showed changes in the intensity of peaks in the region of 917.00–674.33 cm^{-1}, which can be attributed to the presence of quartz as an impurity in the bentonite, as well as the contribution of OH groups.

Results of adsorption experiments

Investigation of the effect of pH value

Figure 4 shows the effect of pH value on the adsorption capacity and removal efficiency of Cr(III) ions from the synthetic aqueous solution. As shown in Figure 4., the pH value has a significant influence on the metal ion adsorption process. At a pH value of 2, the lowest adsorption capacity of 417.627 mg/g for Cr(III) ions was recorded, while the highest adsorption capacity and metal removal efficiency were observed at pH 5, amounting to 498.966 mg/g and 99.793%, respectively. The lower adsorption capacity is probably caused by the increased

concentration of H^+ ions, whereas the higher efficiency of heavy metal removal at higher pH values can be explained by the fact that, as the pH increases, the concentration of H^+ ions decreases and the active sites of the clay undergo deprotonation, thus attracting positively charged ions through electrostatic interactions (Noyan,2007).

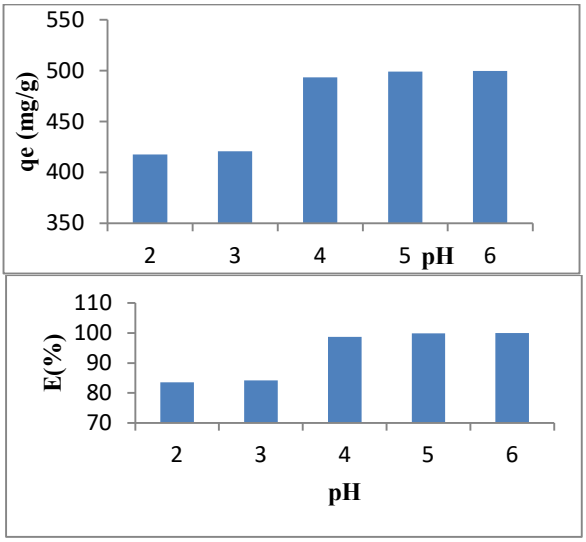

Fig 4. Effect of pH value
a) on the adsorption capacity b) removal efficiency

The obtained results are consistent with previously reported studies on the influence of pH on the adsorption of heavy metal ions on various clays (Jiang *et al*.,2010). Considering these results and the effect of pH on ion adsorption, further experiments were conducted at pH 5 to avoid precipitation in the form of hydroxides (Zhirong,2011).

Effect of initial concentration

Figure 5. shows the effect of the initial concentration on the adsorption capacity and removal efficiency of Cr(III) ions from the synthetic aqueous solution.

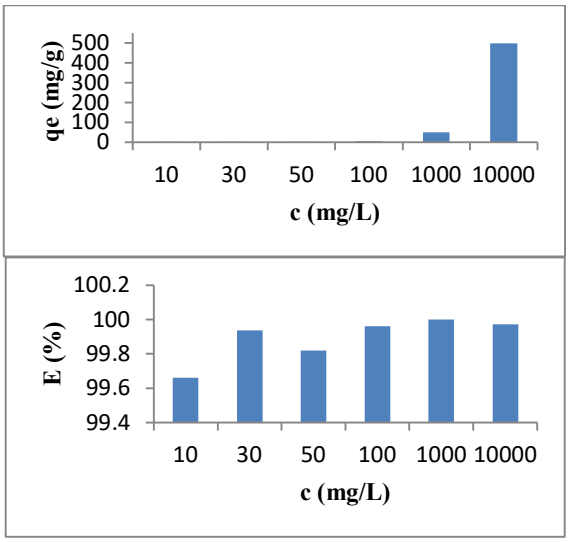

Fig 5. Effect of concentration a) on the adsorption capacity b) removal efficiency

The results show that with an increase in the initial metal concentration, the adsorption capacity also increases, reaching a maximum of 499.862 mg/g at a concentration of 10000 mg/L, which corresponds to an adsorption efficiency of 99.97%.

Effect of contact time

Figure 6 shows the effect of contact time on the adsorption capacity and removal efficiency of Cr(III) ions from synthetic and real aqueous solutions.

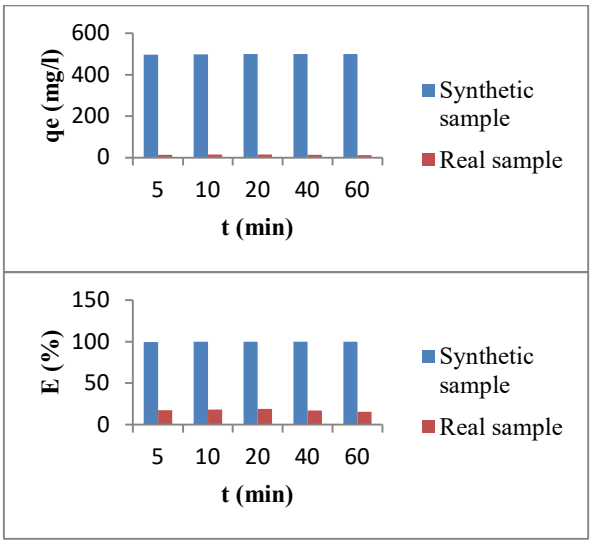

Fig 6. Effect of contact time a) on the adsorption capacity b) removal efficiency

The adsorption process occurred rapidly during the first few minutes, after which equilibrium was established, and the adsorption rate remained constant with further increases in contact time. The maximum removal efficiency of Cr(III) ions was 99.972% for the synthetic sample and 14.4% for the real sample at 60 min. The rapid removal rate can be explained by the fact that, at the beginning of the adsorption process, many active sites are available, which become occupied after a certain period once equilibrium is reached (Han,2006).

Effect of adsorbent mass

Figure 7. shows the effect of adsorbent mass on adsorption capacity and removal efficiency of Cr(III) ions from synthetic and real aqueous solutions. As can be seen from Figure 7a)., increasing the mass of the adsorbent increases the adsorption capacity of the synthetic sample, while increasing the mass of the adsorbent in the real sample decreases the adsorption capacity, which can be explained by the fact that during the adsorption process, the binding sites remain unsaturated. The presented results from Figure 7b). indicate that increasing the mass of the adsorbent leads to a significant increase in the removal efficiency of the examined ions, with a maximum efficiency for Cr(III) ions achieved at an adsorbent mass of 1 g for both synthetic and real sample. It is expected that increasing the adsorbent mass provides more binding sites on the adsorbent surface available for interaction

with metal ions, resulting in higher efficiency of metal ion removal from aqueous solutions (Bohli *et al*.,2013).

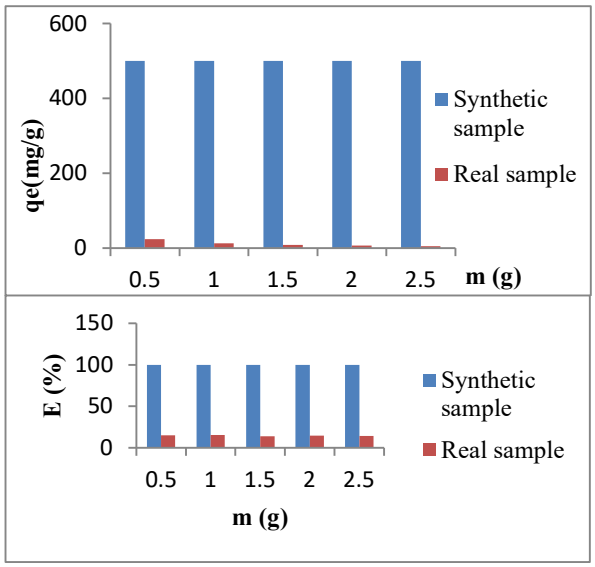

Fig 7. Effect of adsorbent mass a) on the adsorption capacity b) removal efficiency

Effect of temperature

Figure 8. shows the effect of temperature on the adsorption capacity and removal efficiency of Cr(III) ions from synthetic and real aqueous solutions.

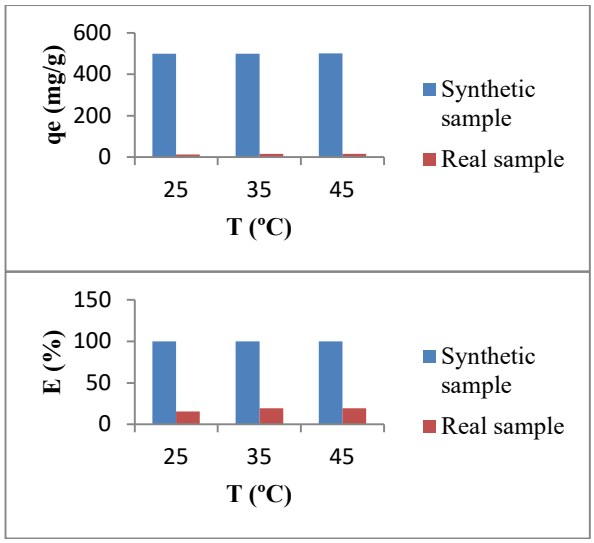

Fig 8. Effect of temperature a) on the adsorption capacity b) removal efficiency

As can be seen in Figure 8, the highest efficiency was achieved at a temperature of 45°C, with a maximum removal efficiency of Cr(III) of 99.992% for the synthetic sample and 18.870% for the real sample. Based on these results, it can be concluded that the adsorption.

The process for Cr(III) ions is endothermic (Afroze,2018).

Adsorption isotherm and models

Adsorption isotherms are very important for evaluating the maximum adsorption capacity of an adsorbent and for describing the interaction between the adsorbate and the adsorbent (Igwe, 2007). To assess the adsorption capacity of bentonite, the adsorption results of the investigated Cr(III) ions at different initial metal concentrations in synthetic aqueous solutions ranging from 10 to 10000 mg/L, and in a real solution with a concentration of 1643.57 mg/L, were analyzed using the Langmuir, Freundlich, and Temkin adsorption isotherm models. By applying the linear forms to the experimental equilibrium adsorption data, the required parameters were calculated using equations (3),(3.1.),(4), and (5), and the obtained results for the synthetic and real samples are presented in Table 3.

Langmuir adsorption isotherm

$$\frac{c_e}{q_e} = \frac{1}{K_L} + \frac{\alpha_L}{K_L} \cdot C_e \quad (3)$$

$$R_L = \frac{1}{1 + K_L \cdot C_o} \quad (3.1)$$

where: q_e (mg/g) – the amount of adsorbate adsorbed on the adsorbent at equilibrium conditions; C_e (mg/dm³) – equilibrium concentration of the adsorbate in the solution; q_{max} (mg/g) – the maximum amount of adsorbate adsorbed per unit mass of adsorbent, i.e., the maximum monolayer adsorption capacity, α_L (dm³/g) and K_L (dm³/mg) – Langmuir constants indicating the adsorption affinity of the adsorbent toward the investigated adsorbate.

Freundlich adsorption isotherm

$$log q_e = \log K_f + \frac{1}{n} \cdot \log C_e \quad (4)$$

where: q_e (mg/g) – the amount of adsorbate adsorbed on the adsorbent at equilibrium conditions; C_e (mg/dm³) – equilibrium concentration of the adsorbate in the solution; K_f ((mg/g)(dm³/mg)$^{1/n}$) – Freundlich adsorption constant; and n (dimensionless) – Freundlich constant indicating the intensity of the adsorption process and reflecting the surface heterogeneity.

Temkin adsorption isotherm

$$q_e = \frac{RT}{b} \ln K_t \; C_e \quad (5)$$

where: q_e(mg/g) – amount of adsorbate adsorbed onto the adsorbent at equilibrium conditions, C_e(mg/dm³) – equilibrium concentration of the adsorbate in the solution, R(8.314 J/mol·K) – universal gas constant, T(K)–absolute temperature, K_t(dm³/g) and b(J/mol) – Temkin constants corresponding to the adsorbate–adsorbent interaction and the heat of adsorption, respectively.

The best fit of the isotherm models with the experimental data was determined based on the correlation coefficient R^2. According to the data presented in Table 3., it can be observed that the experimental results for the removal of Cr(III) ions from the synthetic aqueous solution fit well with the Langmuir isotherm model, where the correlation coefficient R^2=1 for the investigated concentration range. The Temkin isotherm model also showed a good fit with the experimental data, with the highest correlation coefficient R^2 obtained at a concentration of 10 mg/L. The Freundlich isotherm model, which describes adsorption on a heterogeneous surface, gave the poorest results, with correlation coefficient values lower than those of the Langmuir and Temkin models (Gadd,2009). A good

agreement with the experimental results for the real sample was obtained using the Temkin and Freundlich adsorption models, where the correlation coefficient was R^2=1 for the Temkin model and R^2=0.998 for the Freundlich model.

Table 3: Values of adsorption isotherms for synthetic and real samples

Conc. (mg/L)	Isotherm model- **Freundlich model**			
	1/n	K_f (mg/g)	R^2	
10	-0.006	2.047	0.9656	
30	-0.0028	1.483	0.8576	
50	-0.0031	2.476	0.9847	
100	-0.0011	4.980	0.9265	
1000	$-2.00\cdot10^{-5}$	4.886	0.8767	
10,000	-0.0014	500.841	0.9329	
Conc. (mg/L)	Isotherm model- Langmuir model			
	Q_m (mg/g)	K (dm^3/mg)	R_L	R^2
10	0.4931	0.0003945	1.00394	1
30	1.4861	0.0004458	1.0133	1
50	2.4820	0.000496	1.0248	1
100	4.9850	$1.50\cdot10^{-4}$	1.0100	1
1000	5	$3.5\cdot10^{-6}$	1.0003	1
10,000	500	$2.0\cdot10^{-2}$	$2.01\cdot10^{2}$	1
Conc. (mg/L)	Isotherm model- **Temkin model**			
	B (J/mol)	A (l/mg)	R^2	
10	0.4883	0.993	0.9661	
30	1.4833	0.9971	0.8584	
50	2.4766	0.9968	0.9848	
100	4.9811	0.9988	0.9267	
1000	4.9990	0.9990	0.8760	
10,000	500.830	0.9985	0.9330	
Real sample				
Conc. (mg/L)	Isotherm model- **Freundlich model**			
	1/n	Kf (mg/g)	R^2	
1643.57	-4.835	2.013	0.998	
Conc. (mg/L)	Isotherm model- **Langmuir model**			
	Q_m (mg/g)	K (dm^3/mg)	R_L	R^2
1643.57	2.398	-1130.095	-1857828.1	0.996
Conc. (mg/L)	Isotherm model- **Temkin model**			
	B (J/mol)	A (l/mg)	R^2	
1643.57	504.03	0.873	1	

The values of the 1/n parameter of the Freundlich adsorption isotherm were negative for each concentration of both the synthetic and real samples at the initial concentrations of the analyzed metals, indicating that the adsorbent has a high degree of heterogeneity.

Kinetic models

To examine the kinetics of the adsorption process of Cr(III) ions on bentonite, three models were used: the pseudo-first-order model, the pseudo-second-order model and the intraparticle model. All models were calculated using equations (7),(8),(9) and (10), and the results obtained by nonlinear regression for the parameters of the kinetic models, using the Polymath program for different initial concentrations of Cr(III) ions as well as the actual concentration of the real sample, are presented in Table 4.

Pseudo-first-order model

$$\frac{dq_t}{d_t} = k_1(q_e - q_t) \quad (7)$$

where: q_t represents the amount of adsorbate bound at time t (mg/g); t – time (min); q_e – amount of adsorbate bound at equilibrium conditions.

Pseudo-second-order model

$$\frac{dq_t}{dt} = k_2(q_e - q_t)^2 \quad (8)$$

where: q_e and q_t have the same meaning as in the pseudo-first-order model, and k_2 (g/mg·min) is the rate constant of the pseudo-second-order model.

Intraparticle diffusion model

$$q_t = k_d t^{1/2} + I \quad (9)$$

where the intercept I refers to the thickness of the boundary layer on the adsorbent surface, and k_d is the rate constant of the intraparticle diffusion model.

n^{th} order model

$$\frac{dq_t}{dt} = k(q_e - q_t)^n \quad (10)$$

where: q_t represents the amount of adsorbate bound at time t (mg/g); t – time (min); q_e – amount of adsorbate bound at equilibrium conditions,k–n^{th}order rate constant (g/mg·min), n-order of adsorption kinetics.

Based on the obtained results, it can be concluded that there is a good agreement with interparticle diffusion model (R^2>0.7) and the pseudo-first-order model (R^2>0.5) at all concentrations of the synthetic sample, which implies that the rate of occupation of active sites is proportional to the number of unoccupied sites, with the adsorbate binding to a single active site. Based on the results for the real sample, it can also be concluded that the adsorption process follows the interparticle diffusion model, since the correlation coefficient (R^2) was the highest for this model, with a value of R^2=0.796. Additionally, a high correlation coefficient was obtained for the n^{th} order reaction model for the real sample, where the correlation coefficient was also R^2=0.796.

Table 4. Values of kinetic models

Conc. (mg/L)	Pseudo-first-order model		
	k_1 (l/min)	qe (mg/g)	R^2
10	0.236	0.492	0.584
30	0.236	1.484	0.583
50	0.235	2.469	0.581
100	0.236	4.950	0.580
1000	0.235	49.568	0.579
10,000	0.235	495.228	0.581
Conc. (mg/L)	**Pseudo-second-order model**		
	k_2 (g/mg·min)	qe (mg/g)	R^2
10	0.417	0.526	0.579
30	0.139	1.578	0.579
50	0.087	2.572	0.578
100	0.044	5.102	0.579
1000	0.0040	50.033	0.578
10,000	0.0004	516.023	0.579
Conc. (mg/L)	**Intraparticle diffusion model**		
	K_d (mg/g·min$^{(1/2)}$)	I (mg/g)	R^2
10	-0.0196	0.096	0.777
30	-0.059	0.291	0.777
50	-0.098	0.486	0.776
100	-0.198	0.976	0.777
1000	-1.985	9.786	0.776
10,000	-19.787	97.612	0.777
	Real sample		
Conc. (mg/L)	**Pseudo-first order model**		
	K_1 (l/min)	q_e (mg/g)	R^2
1643.57	0.204	14.085	0.766
Conc. (mg/L)	**Pseudo-second-order model**		
	k_2 (g/mg·min)	qe (mg/g)	R^2
1643.57	0.0078	18.714	0.691
Conc. (mg/L)	**Intraparticle diffusion model**		
	K_d (mg/g·min$^{(1/2)}$)	I (mg/g)	R^2
1643.57	-5.21	14.516	0.796
Conc. (mg/L)	**n order model**		
	K (g/mg·min)	q_e (mg/g)	R^2
1643.57	0.521	14.514	0.796

Table 5. presents the values of the thermodynamic parameters of the adsorption process for Cr(III) ions at three different temperatures, for both the synthetic and real samples.

Table 5. Values of thermodynamic parameters for the synthetic and real samples

Temperature (ºC)	**Termodynamic parameters syntetic sample**		
	ΔG^0 (kJ/mol)	ΔS^0 (J/mol·K)	ΔH^0 (J/mol)
25	-20.346		
35	-21.009	66.304	-587.567
45	-21.679		
Temperature (ºC)	**Termodynamic parameters real sample**		
	ΔG^0 (kJ/mol)	ΔS^0 (J/mol·K)	ΔH^0 (J/mol)
25	10.003		
35	10.342	-33.987	-122.534
45	10.682		

Based on the values given in the table, it can be concluded that the enthalpy (ΔH^o) values for both the synthetic and real samples are negative, indicating that the process is exothermic and that bentonite has a high affinity for these metal ions. The negative Gibbs energy (ΔG^o) values for the synthetic sample indicate that the process is spontaneous and that the heavy metal ions have a strong affinity toward the adsorbent (Dim,2020). Positive Gibbs energy values were recorded for the real sample, suggesting that the process is not spontaneous in this case. The increase in Gibbs energy with rising temperature for both samples indicates that the adsorption process is feasible even at higher temperatures. The positive entropy change (ΔS^o) for the synthetic sample suggests increased randomness and a rise in the degrees of freedom at the solid–liquid interface during metal ion binding, while the negative value indicates a decrease in randomness (Akar *et al.*,2013). Arshadi *et al.* (2014) explained the positive entropy value as a result of energy redistribution between the adsorbate and the adsorbent.

Column adsorption

The experiments on the adsorption of Cr(III) ions from their solutions were carried out in a fixed-bed column with an adsorbent layer height of 5 cm and a solution layer height of 22 cm. Figure 9. shows the breakthrough curve for Cr(III) ions at a time and volume of 1 dm³, pH 5, with a concentration of 10000 mg/L for the synthetic solution and 1643.57 mg/L for the real sample.

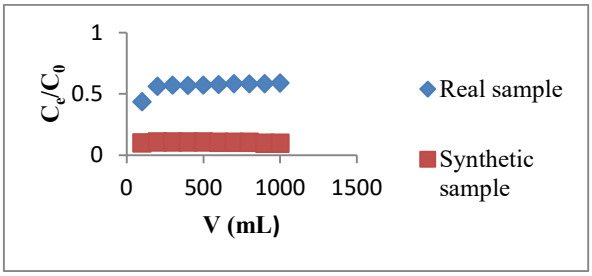

Fig 9. Breakthrough curve for the adsorption of Cr(III) ions

As can be seen from the graph, the breakthrough point for Cr(III) ions occurred at the first 100 mL of the solution and approximately 1 min for the synthetic sample, with further passage of the ion solution, the plateau of the breakthrough curve increased significantly until 800 mL of solution had passed, when the value of 0.103 was reached, after which a slight decrease was observed. The adsorption process of the real sample occurred rapidly at a flow rate of 40 mL/min, with the breakthrough point appearing immediately after passing 100 mL of the solution. With further passage of the solution, the plateau of the formed curve increased and reached a value of 0.587, indicating that the adsorption process took place rapidly but did not reach a relative equilibrium value, which suggests that the process was not yet completely finished and continued at a negligible rate. This can be explained by the Faten *et al*.,(2022), who showed that breakthrough curves at lower flow rates lead to slower equilibrium establishment but higher removal efficiency due to the longer contact time available.

CONCLUSIONS

In this study, bentonite was used as an inexpensive and easily available adsorbent for the adsorption of Cr(III) ions, proving to be highly effective in removing Cr(III) ions from galvanic wastewater. The bentonite sample was characterized using FTIR, SEM-EDS, and BET analyses, and the results showed a large specific surface area and an irregular structure with large pores, which is essential for the adsorption process. The adsorption of Cr(III) ions was evaluated by examining several parameters, including pH value, initial concentration, adsorbent mass, and contact time. The results indicated that the adsorption process occurs rapidly and that increasing the concentration leads to higher adsorption capacity and removal efficiency for both tested metal samples (E > 90%). The Langmuir and Temkin models showed the best fit with the experimental values within the studied concentration range, while the best agreement with kinetic models was achieved using the pseudo-first-order model for both samples, as well as the n order for the real sample. The column experiment results showed that the adsorption process proceeds at a high rate, with the breakthrough point occurring after the first 100 mL of the passed solution.

REFERENCES

Afroze, S., Sen, T. K. (2018). A Review on Heavy Metal Ions and Dye Adsorption from Water by Agricultural Solid Waste Adsorbents. *Water, Air, & Soil Pollution, 229(7), 225. DOI: 10.1007/s11270-018-3869-z.*

Ahmetović, M., Šestan, I., Odobašić A., Papraćanin, E. (2024). Bentonite as a Potential Adsorbent for the Removal of Copper Ions from the Galvanic Industry Wastewater. *Advanced Technologies, Systems, and Applications IX, Springer*. DOI: 10.1007/978-3-031-71694-2_47.

Ahmetović, M., Šestan, I., Odobašić, A., Papraćanin, E., Keran, H., Đozić, A. and Junuzović, H., (2024). The potential of bentonite as a low-cost adsorbent for the removal of heavy metal ions from multicomponent aqueous systems of the galvanic industry. *International Research Journal of Pure and Applied Chemistry, 25(2), pp.28-39.* DOI: 10.9734/irjpac/2024/v25i2848.

Akar, S.T., Yilmazer, D., Celik, S., Balk, Y.Y., Akar T., (2013). On the utilization of a lignocellulosic waste as an excellent dye remover: Modification, characterization, and mechanism analysis, *Chemical Engineering Journal 229:257-266.* DOI: 10.1016/j.cej.2013.06.009.

Arshadi, M., Amiri, M. J., Mousavi, S. (2014). Kinetic, equilibrium and thermodynamic investigations of Ni(II), Cd(II), Cu(II), and Co(II) adsorption on barley straw ash.*Water resources and Industry (6), 1-17.* DOI: 10.1016/j.wri.2014.06.001.

Bohli, T., Villaescusa, I., Ouedern, A. (2013). Comparative Study of Bivalent Cationic Metals Adsorption Pb(II), Cd(II), Ni(II), and Cu(II) on Olive Stones Chemically Activated Carbon. *Journal of Chemical Engineering & Process Technology, (4)04.* DOI: 10.4172/2157-7048.1000158.

Daković, A., Tomašević-Čanović, M., Dondur,V., Stojšić, D., Rottinghous, G., (2001). *Zeolites and mesoporous materials at the dawn of the 21st century* in Proceedings of the 13th International Conference. Montpellier, France. DOI: 10.1016/S1387-1811(03)00365-2.

Dengbing, W., Dingsheng, W., Anfang, W., Jun G., Chengling, P, Ze, M., Quan, F. (2025). Scalable, high flux of electrospun nanofibers membrane for rapid adsorption-reduction synergistic removal of Cr(VI) ions in wastewater. *Separation and Purification Technology, Vol. 360 (2), 130747,1383-5866.* DOI: 10.1016/j.seppur.2024.130747.

Dhaouadi, F., Sellaoui, L., Chávez-González, B., Elizabeth Reynel-Ávila H., DiazMuñoz L. L.,Mendoza-Castillo D.I., Petriciolet, A.B., Lima,E.C., Picazo J.C.T., Ben Lamine, A.B., (2021).Application of a heterogeneous physical model for the adsorption of Cd^{2+}, Ni^{2+}, Zn^{2+} and Cu^{2+} ions on flamboyant pods functionalized with citric acid. *Chemical Engineering Journal,417:127975.* DOI: 10.1007/s11356-021-12832-x.

Dim, P.E, Olu, C.S, Okafor, O.J (2020) .Kinetic and thermodynamic studies of the adsorption of Cu (II) and Cr (VI) ions from an industrial effluent on a kaolinite clay, *Journal of Chemical Technology and Metallurgy 55(5)1057-1067.*

Faten B.H., Brooke K.M.B. (2022). Fixed-bed column study of phosphate adsorption using immobilized phosphate-binding protein. *Chemosphere 295, 133908*. DOI: 10.1016/j.chemosphere.2022.133908.

Fonseca, M.G., Oliveira, M.M., Arakaki, L.N.H (2006). Removal of cadmium, zinc, manganese and chromium cations from aqueous solution by a clay mineral, *Journal of Hazardous Materials 137(1), 288–292. DOI: 10.1016/j.jhazmat.2006.02.001.*

Gadd, G. M. (2009). Biosorption: critical review of scientific rationale, environmental importance and significance for pollution treatment. *Journal of Chemical Technology & Biotechnology, 84(1), 13–28.* DOI: 10.1002/jctb.1999.

Gandhi, D., Bandyopadhyay, R., Soni, B. (2022). Naturally occurring bentonite clay: Structural augmentation, characterization and application as

catalyst. *Elsevier, Materials Today:Proceedings, 57 (1), 194-201*. DOI: 10.1016/j.matpr.2022.02.346.

Gaoqian, Y., Kezhuo, L., Jingzhe, Z., Long, D., Yage, L., Guodong, Y., Liang, H., Faliang, L., Haijun, Z., Shaowei, Z. (2024). Construction of bionic sea urchin-like $ZnFe_2O4/Bi_2S_3$ heterojunction for microwave-induced catalytic reduction of Cr(VI): Performance and mechanism insights, *Chemical Engineering Journal, Vol. 488. DOI: 10.1016/j.cej.2024.150766*

Gholamifard,H., Rasul,M.G., Rahideh,H., Azari, A., Abbasi, M., Karami, R. (2023). Experimental and numerical analysis of oily wastewater treatment using low-cost mineral adsorbent in a single and multi-fixed bed column, *Chemical Engineering Journal Advances (16) Article 100551*. DOI: 10.1016/j.ceja.2023.100551.

Han, R., Zou, W., Zhang, Z., Shi, J., Yang, J. (2006).Removal of copper(II) and lead(II) from aqueous solution by manganese oxide coated sand. *Journal of Hazardous Materials, 137(1), 384–395.* DOI: 10.1016/j.jhazmat.2006.02.021.

Igwe, C.J., Abia, A.A. (2007). Equilibrium sorption isotherm studies of Cd(II), Pb(II) and Zn(II) ions detoxification from waste water using unmodified and EDTA-modified maize husk, *Electronic Journal of Biotechnology 10(4),0717-3458*. DOI: 10.2225/vol10-issue4-fulltext-15.

Jiang, M.Q., Jin, X.Y., Lu, X.Q., Chen Z.L. (2010). Adsorption of Pb(II), Cd(II), Ni(II) and Cu(II) onto Natural Kaolinite Clay. *Desalination, 252, 33-39.* DOI: 10.1016/j.desal.2009.11.005

Joyel, P., Ahsan, Q., Sandeep, S.A., Sabu, T., Alain, D. (2024) Chitosan-based aerogels: A new paradigm of advanced green materials for remediation of contaminated water. *Carbohydrate Polymers, Vol. 338, 122198, 0144-8617*. DOI: 10.1016/j.carbpol.2024.122198

Kejin, Y., Lina Y., Siyu, Z., Ning, Z. (2025). Nanocellulose-based aerogels for the adsorption and removal of heavy-metal ions from wastewater: A review, *Materials Today Communications, Vol. 43,111744, 2352-4928.* DOI: 10.1016/j.mtcomm.2025.111744.

Kovo G. A, Folasegun A.D. (2015). Potential of a low-cost bentonite for heavy metal abstraction from binary component system, *Journal of Basic and Applied Science (4) 1-13.* DOI: 10.1016/j.bjbas.2015.02.002.

Maged, A., Kharbish, S., Ismael S.I., Bhatnagar A. (2020). Characterization of activated bentonite clay mineral and the mechanisms underlying its sorption for ciprofloxacin from aqueous solution. *Environmental Science and Pollution Research, 27:32980–32997*. DOI: 10.1007/s11356-020-09267-1

Noreen S., Khalid U., Ibrahim S. M., Javed T., Ghani A., Naz S., Iqbal,M. (2020). ZnO, MgO and FeO adsorption efficiencies for direct sky Blue dye: equilibrium, kinetics and thermodynamics studies. *Journal of Material Research and Technology:9(3)5881–5893.* DOI: 10.1016/j.jmrt.2020.03.115.

Noyan H., Önal M., Sarıkaya Y. (2007). The effect of sulphuric acid activation on the crystallinity, surface area, porosity, surface acidity, and bleaching power of a bentonite. *Food Chemistry 105(1)156–163*. DOI: 10.1016/j.foodchem.2007.03.060.

Petrović,R., Gajić,D., Obrenović, Z., Bodroža, D., Popadić,N.,Davidović,D., Ćulumović, M., (2019). Kinetics of Cr(VI) adsorption from aqueous medium onto bentonite,*Glasnik hemičara, tehnologa i ekologa Republike Srpske (15) 9-16.* DOI: 10.7251/GHTE1915009P.

Sher, F., Hanif, K., Rafey,A., Khalid, U., Zafar,A., Ameen,M., Lima,E.C (2021). Removal of micropollutants from municipal wastewater using different types of activated carbons„*Journal of Environmental Management, 278 (2) 111302.* DOI: 10.1016/j.jenvman.2020.111302.

Tadesse, S.H. (2022). Application of Ethiopian bentonite for water treatment containing zinc. *Journal of Emerging Contaminants 8 (1): 113-122*. DOI: 10.1016/j.emcon.2022.02.002.

Vhahangwele, M., Mugera, W.G., Tholiso, N. (2014). Defluoridation of drinking water using Al^{3+} modified bentonite clay: optimization of fluoride adsorption conditions*, Toxicological & Environmental Chemistry, 96(9),1294-1309.* DOI: 10.1080/02772248.2014.977289.

Wael,I. M., Ali, E.N., Ahmed, M.K., Niroshika, P., Balal, Y., Ronggui, T., Shengsen, W., Yanjiang, C., Scott, X.C. (2023). Biogeochemical behaviour and toxicology of chromium in the soil-water-human nexus: A review, *Chemosphere, Vol. 331, 138804, 0045-6535*. DOI: 10.1016/j.chemosphere.2023.138804.

Wu, Y., Pang, H., Liu, Y., Wang, X., Yu, S., Fu, D., et al. (2019). Environmental remediation of heavy metal ions by novel-nanomaterials: a review. Environmental Pollution 246, 608–620. DOI: 10.1016/j.envpol.2018.12.076.

Saghir,Y., Chaoui,A., Farsad,S., Ben H.A, Amjlef,A., Benafqir,M., Alem,E.N., Ez-zahery, M. (2025). Improving the adsorption efficiency of a low-cost natural adsorbent for the removal of an organic pollutant: optimization and mechanism study. *Materials Advances, Volume 6, (4), Pg 4857-4873*. DOI: 10.1039/d5ma00253b.

Zhirong L., Azhar, U. M., Zhanxue S. (2011). FT-IR and XRD analysis of natural Na-bentonite and Cu(II)-loaded Na-bentonite. *Spectrochim Acta A Mol Biomol Spectrosc.79(5),1013-6*. DOI:10.1016/j.saa.2011.04.013.

Summary/Sažetak

Prisustvo teških metala poput hroma u vodotocima može da dovede do različitih zdravstvenih problema kod ljudi, ali i životinja. Zbog negativnog učinka prije ispuštanja u vodotoke otpadne vode obogaćene hromom potrebno je pročistiti. U ovom radu proučavana je mogućnost upotrebe bentonita kao adsorbensa za uklanjanje hroma iz otpadnih voda galvanske industrije. Najprije je urađena fizičko-hemijska karakterizacija korištenog bentonita, a zatim je ispitan uticaj procesnih parametara poput pH vrijednosti, koncentracije, mase i vremena. Na osnovu dobijenih podataka urađene su i adsorpcijske izoterme, kao i kinetički modeli i termodinamika. Svi provedeni eksperimenti su rađeni saržnim sistemom i sistemom u koloni. Rezultati su pokazali da se bentonit može koristiti kao jeftini adsorbens za efikasno uklanjanje jona hroma iz otpadne vode galvanske industrije, te da pri pH 5, masi od 1g postiže najveća efikasnost uklanjanja (99.97%). Langmuirov i Temkinov model adsorpcijskih izotermi pokazao je dobro slaganje sa eksperimentalnim vrijednostima (R^2>0.9), dok je najbolje slaganje sa kinetičkim modelom zabilježeno kod pseudo-prvog modela.